Mass spectra of neutral mesons K_0,π_0,η,η' at finite magnetic field, temperature and quark chemical potential

Jie Mei,[1,2] Tao Xia,[3] and Shijun Mao[1,*]

[1]*School of Physics, Xi'an Jiaotong University, Xi'an, Shaanxi 710049, China*
[2]*School of Physics Sciences, University of Chinese Academy of Sciences, Beijing 100049, China*
[3]*College of Advanced Interdisciplinary Studies, National University of Defense Technology, Changsha, Hunan 410073, China*

(Received 13 December 2022; accepted 30 March 2023; published 14 April 2023)

The mass spectra of neutral mesons K_0, π_0, η, η' on the temperature-quark chemical potential (T-μ) plane under a constant magnetic field is investigated in the $SU(3)$ Nambu-Jona-Lasinio model. As a Goldstone boson of chiral symmetry breaking, the mass of K_0 meson generally increases with temperature and/or quark chemical potential, and we observe two kinds of mass jumps of the K_0 meson in medium, one of which is induced by the mass jump of constituent quarks and the other by the magnetic field. Due to the breaking of isospin symmetry between u and d quarks in the presence of magnetic fields, a flavorless neutral meson mixing involving the $\pi_0 - \eta - \eta'$ mesons occurs (in the isospin symmetric case the mixing involves only $\eta - \eta'$) and a rich structure is found in the mass spectra of these mesons. For instance, the π_0 mass is influenced by the strange quark. A change in the slope of the μ dependency of the π_0 mass at high μ and vanishing T can be associated with the crossing of the threshold of two times of strange quark mass. In the finite T case, this behavior is changed into the appearance of a critical chemical potential at which a jump over the threshold of $2m_s$ occurs. The mass ordering of π_0, η, η' mesons varies in medium, due to their mass jumps, which are induced by the mass jump of constituent quarks or the magnetic field.

DOI: 10.1103/PhysRevD.107.074018

I. INTRODUCTION

The study of hadron properties in QCD medium is important for our understanding of strong interaction matter, due to its close relation to QCD phase structure and relativistic heavy ion collision. The chiral symmetry breaking leads to the rich meson and baryon spectra, and the $U_A(1)$ anomaly explains the nondegeneracy of η and η' mesons [1]. The mass shift of hadrons will enhance or reduce their thermal production in relativistic heavy ion collisions, such as the kaon yields and ratios [2–5].

It is widely believed that the strongest magnetic field in nature may be generated in the initial stage of relativistic heavy ion collisions. The initial magnitude of the field can reach $eB \sim (1\text{–}100)m_\pi^2$ in collisions at the Relativistic Heavy Ion Collider and the Large Hadron Collider [6–10], where e is the electron charge and m_π the pion mass in vacuum. In recent years, the study of magnetic field effects on the hadrons has attracted much attention. As the Goldstone bosons of the chiral (isospin) symmetry breaking, the properties of neutral (charged) pions at finite magnetic field, temperature and density are widely investigated [11–55]. Another interesting issue is the charged rho meson, which is related to the electromagnetic superconductivity of the QCD vacuum [21,25,56–72]. Furthermore, there are some other works involving K, η, η', and ϕ mesons [51,73–76], heavy mesons [77–88], and baryons [89–95] in the magnetic field.

In the previous study, the effects of a magnetic field on K, η, and η' mesons are mostly considered in vacuum, with vanishing temperature and density [51,73–75]. Our current work focuses on the mass spectra of neutral mesons K_0, $\bar{K}_0$, π_0, η, and η' mesons at finite magnetic field, temperature, and density, which are related to the restoration of chiral symmetry and the $U_A(1)$ anomaly. When the magnetic field is of strength comparable with the strong interaction energy scale, such as $eB \sim m_\pi^2$, the quark structure of hadrons should be taken into account. We apply the three flavor Nambu-Jona-Lasinio (NJL) model at quark level [96–99], where quarks are treated in mean field level and mesons are

*maoshijun@mail.xjtu.edu.cn

the quantum fluctuations constructed from the quark bubble. The electromagnetic interaction of the charged constituent quarks leads to a sensitive dependence of the neutral meson properties on the external electromagnetic fields, for instance, the meson mass jump induced by dimension reduction of the constituent quarks [33–35,41–43,45,46], and the $\pi_0-\eta-\eta'$ mixing due to the breaking of isospin symmetry between u and d quarks [75,100], in magnetic fields.

The rest of paper is arranged as follows. We introduce the magnetized $SU(3)$ NJL model and derive the formula for quarks and neutral mesons mass spectra in Sec. II. The numerical results and analysis of neutral meson masses at finite magnetic field, temperature, and baryon chemical potential are presented in Sec. III. The summary and outlook are in Sec. IV.

II. FORMALISM

The three-flavor NJL model under external magnetic field is defined through the Lagrangian density,

$$\begin{aligned}\mathcal{L}&=\bar{\psi}(i\gamma^\mu D_\mu-\hat{m}_0)\psi+\mathcal{L}_S+\mathcal{L}_{KMT},\\ \mathcal{L}_S&=G\sum_{\alpha=0}^{8}[(\bar{\psi}\lambda_\alpha\psi)^2+(\bar{\psi}i\gamma_5\lambda_\alpha\psi)^2],\\ \mathcal{L}_{KMT}&=-K[\det\bar{\psi}(1+\gamma_5)\psi+\det\bar{\psi}(1-\gamma_5)\psi].\end{aligned}\tag{1}$$

The covariant derivative $D_\mu=\partial_\mu-iQA_\mu$ couples quarks with electric charge $Q=\mathrm{diag}(Q_u,Q_d,Q_s)=\mathrm{diag}(2/3e,-1/3e,-1/3e)$ to a gauge field $\mathbf{B}=\nabla\times\mathbf{A}$. Here, we consider magnetic field in z direction by setting $A_\mu=(0,0,xB,0)$ in Landau gauge. $\hat{m}_0=\mathrm{diag}(m_0^u,m_0^d,m_0^s)$ is the current quark mass matrix in flavor space. The four-fermion interaction $\mathcal{L}_S$ represents the interaction in scalar and pseudoscalar channels, with Gell-Mann matrices $\lambda_\alpha,\alpha=1,2,\ldots,8$ and $\lambda_0=\sqrt{2/3}\mathbf{I}$. The six-fermion interaction or Kobayashi-Maskawa-'t Hooft term $\mathcal{L}_{KMT}$ is related to the $U_A(1)$ anomaly [101–105].

It is useful to convert the six-fermion interaction into an effective four-fermion interaction in the mean field approximation, and the Lagrangian density can be rewritten as [100]

$$\begin{aligned}\mathcal{L}=\bar{\psi}(i\gamma^\mu D_\mu-\hat{m}_0)\psi&+\sum_{a=0}^{8}[K_a^-(\bar{\psi}\lambda^a\psi)^2+K_a^+(\bar{\psi}i\gamma_5\lambda^a\psi)^2]+K_{30}^-(\bar{\psi}\lambda^3\psi)(\bar{\psi}\lambda^0\psi)+K_{30}^+(\bar{\psi}i\gamma_5\lambda^3\psi)(\bar{\psi}i\gamma_5\lambda^0\psi)\\&+K_{03}^-(\bar{\psi}\lambda^0\psi)(\bar{\psi}\lambda^3\psi)+K_{03}^+(\bar{\psi}i\gamma_5\lambda^0\psi)(\bar{\psi}i\gamma_5\lambda^3\psi)+K_{80}^-(\bar{\psi}\lambda^8\psi)(\bar{\psi}\lambda^0\psi)+K_{80}^+(\bar{\psi}i\gamma_5\lambda^8\psi)(\bar{\psi}i\gamma_5\lambda^0\psi)\\&+K_{08}^-(\bar{\psi}\lambda^0\psi)(\bar{\psi}\lambda^8\psi)+K_{08}^+(\bar{\psi}i\gamma_5\lambda^0\psi)(\bar{\psi}i\gamma_5\lambda^8\psi)+K_{83}^-(\bar{\psi}\lambda^8\psi)(\bar{\psi}\lambda^3\psi)+K_{83}^+(\bar{\psi}i\gamma_5\lambda^8\psi)(\bar{\psi}i\gamma_5\lambda^3\psi)\\&+K_{38}^-(\bar{\psi}\lambda^3\psi)(\bar{\psi}\lambda^8\psi)+K_{38}^+(\bar{\psi}i\gamma_5\lambda^3\psi)(\bar{\psi}i\gamma_5\lambda^8\psi),\end{aligned}\tag{2}$$

with the effective coupling constants

$$\begin{aligned}K_0^\pm&=G\pm\frac{1}{3}K(\sigma_u+\sigma_d+\sigma_s),\\ K_1^\pm=K_2^\pm=K_3^\pm&=G\mp\frac{1}{2}K\sigma_s,\\ K_4^\pm=K_5^\pm&=G\mp\frac{1}{2}K\sigma_d,\\ K_6^\pm=K_7^\pm&=G\mp\frac{1}{2}K\sigma_u,\\ K_8^\pm&=G\mp\frac{1}{6}K(2\sigma_u+2\sigma_d-\sigma_s),\\ K_{03}^\pm=K_{30}^\pm&=\pm\frac{1}{2\sqrt{6}}K(\sigma_u-\sigma_d),\\ K_{08}^\pm=K_{80}^\pm&=\mp\frac{\sqrt{2}}{12}K(\sigma_u+\sigma_d-2\sigma_s),\\ K_{38}^\pm=K_{83}^\pm&=\mp\frac{1}{2\sqrt{3}}K(\sigma_u-\sigma_d),\end{aligned}\tag{3}$$

and chiral condensates

$$\sigma_u=\langle\bar{u}u\rangle,\qquad\sigma_d=\langle\bar{d}d\rangle,\qquad\sigma_s=\langle\bar{s}s\rangle.\tag{4}$$

At finite temperature T, quark chemical potential $\mu=\mu_B/3$, and magnetic field eB, the chiral condensates or effective quark masses $m_u=m_0^u-4G\sigma_u+2K\sigma_d\sigma_s$, $m_d=m_0^d-4G\sigma_d+2K\sigma_u\sigma_s$, $m_s=m_0^s-4G\sigma_s+2K\sigma_u\sigma_d$ are determined by minimizing the thermodynamic potential,

$$\partial\Omega_{\mathrm{mf}}/\partial\sigma_i=0,\qquad i=u,d,s,\tag{5}$$

where the thermodynamic potential in mean field level contains the mean field part and quark part

$$\begin{aligned}\Omega_{\mathrm{mf}}&=2G(\sigma_u^2+\sigma_d^2+\sigma_s^2)-4K\sigma_u\sigma_d\sigma_s+\Omega_q,\\ \Omega_q&=-3\sum_{f=u,d,s}\frac{|Q_fB|}{2\pi}\sum_l\alpha_l\int\frac{dp_z}{2\pi}\Big[E_f\\&\quad+T\ln\left(1+e^{-\frac{E_f+\mu}{T}}\right)+T\ln\left(+e^{-\frac{E_f-\mu}{T}}\right)\Big],\end{aligned}\tag{6}$$

with quark energy $E_f=\sqrt{p_z^2+2l|Q_fB|+m_f^2}$ of flavor $f=u,d,s$, longitudinal momentum p_z and Landau level l, and the degeneracy of Landau levels $\alpha_l=2-\delta_{l0}$.

In vacuum, the chiral symmetry is spontaneously broken. At finite temperature and quark chemical potential, it will become (partially) restored. In nonchiral limit, the pseudocritical temperature of chiral symmetry restoration T^f_{pc} is usually defined through the vanishing second derivative of the effective quark mass, $\frac{\partial^2 m_f}{\partial T^2}|_\mu = 0$. Because of the different current quark masses and/or different electronic charges of up, down, and strange quarks, we have three different chiral restoration phase boundaries in the crossover region, with $T^d_{pc} < T^u_{pc} < T^s_{pc}$. From the numerical calculation, see Fig. 1(a), we find that the chiral restoration phase boundary for light (up and down) quarks is almost coincident with each other $T^d_{pc} \simeq T^u_{pc} = 175$ MeV, and the chiral restoration of strange quarks occurs at higher temperature $T^s_{pc} = 252$ MeV. In low temperature and high baryon chemical potential region, the chiral restoration in light quarks is a first order phase transition, with the quark mass jump. We should be careful of the chiral restoration in strange quark part. Due to the coupling of the three gap equations, the mass jump of light quarks will cause the mass jump of strange quarks. This cannot be classified as the strange quark chiral restoration, which should correspond to a sizable drop in the strange quark mass. For instance, in Fig. 1(b), the chiral restoration of light quarks happens at $\mu = 240.1$ MeV, with a sizable mass jump. There appears a small mass jump for the strange quark. Since its mass continues to be reasonably large, this does not correspond to the strange quark chiral restoration. The strange quark chiral restoration happens at $\mu = 410.2$ MeV, with an abrupt decrease of strange quark mass. In the following context, chiral symmetry restoration and the critical end point (CEP) refer to that of light quarks.

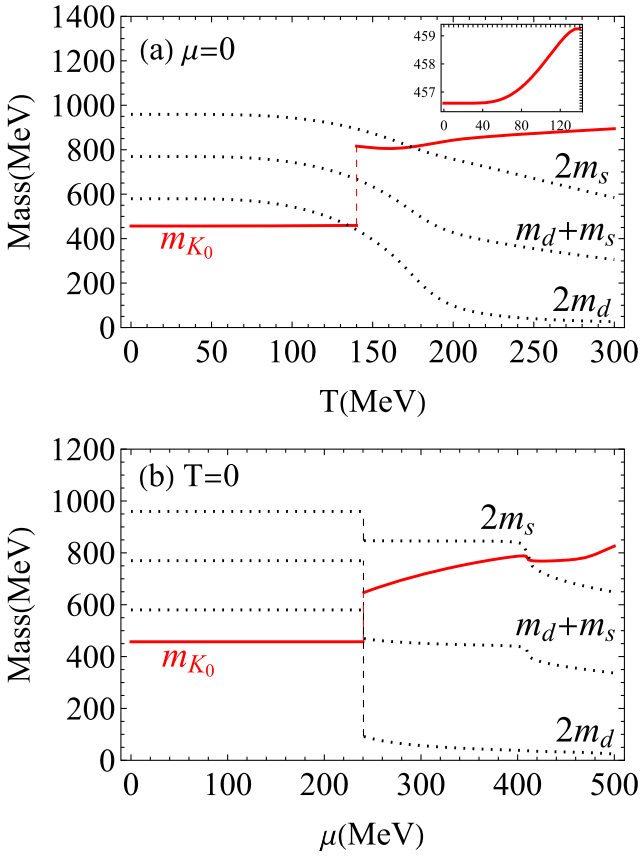

FIG. 1. K_0 meson mass m_{K_0} (red solid lines) and quark mass sum $m_d + m_s$ (black dotted lines) at finite magnetic field $eB = 20m_\pi^2$ with vanishing quark chemical potential $\mu = 0$ in (a) and with vanishing temperature $T = 0$ in (b). The vertical dashed lines are used to denote the sudden mass jumps for quarks (in black) and K_0 meson (in red). To demonstrate the chiral symmetry restoration, we also plot light quark mass $2m_d$ and strange quark mass $2m_s$ (black dotted lines).

In the NJL model, mesons are treated as quantum fluctuations above the mean field. Through the random phase approximation method [28,96–99], the meson propagator can be expressed in terms of the irreducible polarization function or quark bubble,

$$\Pi^P_{M'M}(k) = i\mathrm{Tr}\left[\Gamma^*_{M'} S\left(p + \frac{1}{2}k\right)\Gamma_M S\left(p - \frac{1}{2}k\right)\right], \quad (7)$$

with the quark propagator matrix $S = \mathrm{diag}(S_u, S_d, S_s)$ in flavor space, the meson vertex

$$\Gamma_M = \begin{cases} i\gamma_5\lambda_0, & M = \eta_0 \\ i\gamma_5\lambda_3, & M = \pi_0 \\ i\gamma_5(\lambda_6 \pm i\lambda_7)/\sqrt{2}, & M = K_0, \bar{K}_0 \\ i\gamma_5\lambda_8, & M = \eta_8 \end{cases}, \quad (8)$$

and the trace Tr in spin, color, flavor, and momentum space. For neutral mesons $\pi_0, K_0, \bar{K}_0, \eta, \eta'$, the Schwinger phase arising from quark propagators is canceled, and the meson momentum $k = (k_0, \vec{k})$ itself is conserved.

Let us start from neutral kaon mesons $(K_0, \bar{K}_0)$, which are not mixing with other mesons. The K_0 meson propagator can be written as

$$\mathcal{M}(k_0, \vec{k}) = \frac{2K_6^+}{1 - 2K_6^+\Pi^P_{K_0K_0}(k_0, \vec{k})}, \quad (9)$$

and the mass is determined through the pole equation at zero momentum $\vec{k} = \vec{0}$,

$$1 - 2K_6^+\Pi^P_{K_0K_0}(m_{K_0}, \vec{0}) = 0. \quad (10)$$

Since the K_0 meson is charge neutral, it is affected by the external magnetic field only through the constituent quarks. The formula for the meson propagator is the same as that without a magnetic field except for the consideration of Landau levels in momentum integral. The polarization function is simplified as

$$\Pi^P_{K_0K_0}(k_0,\vec{0}) = J_1^{(d)} + J_1^{(s)} + 2((m_d - m_s)^2 - k_0^2)J_2^{(ds)}(k_0^2), \tag{11}$$

with

$$J_1^{(f)} = 3\sum_l \alpha_l \frac{|Q_f B|}{2\pi}\int \frac{dp_z}{2\pi}\frac{\tanh\frac{E_f+\mu}{2T}+\tanh\frac{E_f-\mu}{2T}}{2E_f}, J_2^{(ds)}(k_0^2) = -3\sum_l \alpha_l \frac{|Q_f B|}{2\pi}\int \frac{dp_z}{2\pi}\frac{1}{8E_sE_d}$$
$$\times\left[\frac{1}{E_s+E_d+k_0}\left(\tanh\frac{E_s-\mu}{2T}+\tanh\frac{E_d+\mu}{2T}\right)+\frac{1}{E_s-E_d+k_0}\left(\tanh\frac{E_d-\mu}{2T}-\tanh\frac{E_s-\mu}{2T}\right)\right.$$
$$\left.+\frac{1}{E_s+E_d-k_0}\left(\tanh\frac{E_d-\mu}{2T}+\tanh\frac{E_s+\mu}{2T}\right)+\frac{1}{E_s-E_d-k_0}\left(\tanh\frac{E_d+\mu}{2T}-\tanh\frac{E_s+\mu}{2T}\right)\right].$$

As Goldstone boson of chiral symmetry restoration, when the constituent quark mass decreases, the kaon mass will generally increase. Therefore chiral symmetry restoration is expected to lead to an intersection between the K_0 mass and the sum of two constituent quark masses, which defines the Mott transition of K_0 meson [106–109]. Based on the polarization function (11), with $p_z = 0$ and lowest Landau level $l = 0$, the integral term $\frac{1}{E_s+E_d-k_0}$ diverges when $k_0 = m_d + m_s$. This infrared divergence will lead to the mass jump of K_0 meson at the Mott transition, as shown in Figs. 1 and 2. It should be noted that when the meson mass reaches the sum of the effective masses of constituent quarks corresponding to higher Landau levels $\sqrt{2l|Q_dB| + m_d^2} + \sqrt{2l|Q_sB| + m_s^2}$ with $l = 1, 2, \ldots$, this infrared divergence still exists. Therefore, when the mass of K_0 meson is large enough, its mass may undergo more than one jump. After the mass jump, K_0 meson will be in a resonant state with finite width. For simplicity, we still use Eq. (10) to derive K_0 meson mass, neglecting the width of meson [35,41,42].

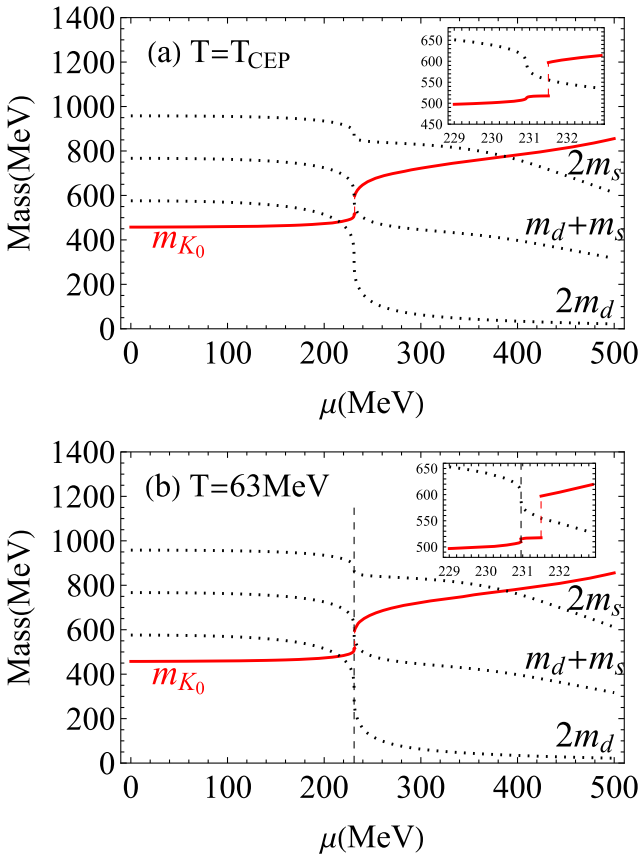

FIG. 2. K_0 meson mass m_{K_0} (red solid lines) and quark mass sum $m_d + m_s$ (black dotted lines) at finite magnetic field $eB = 20m_\pi^2$ around the critical end point. In (a), we fixed temperature at the CEP. Panel (b) is a case of the first order chiral phase transition near CEP. The vertical dashed lines are used to denote the sudden mass jumps for quarks (in black) and K_0 meson (in red). To demonstrate the chiral symmetry restoration, we also plot light quark mass $2m_d$ and strange quark mass $2m_s$ (black dotted lines).

By interchanging two constituent quarks $E_d \leftrightarrow E_s$, we obtain the polarization function of $\bar{K}_0$ meson. When the quark chemical potential is zero, K_0 and $\bar{K}_0$ mesons share the same mass. For finite quark chemical potential, they show mass splitting.

Since the magnetic field breaks the isospin symmetry for u and d quarks, the coupling constants K_{03} and K_{38} are no longer zero. The flavor mixing of $\pi_0 - \eta - \eta'$ happens. Therefore, the meson propagator can be constructed in a matrix form with the random phase approximation method,

$$\mathcal{M} = 2K^+(1 - 2\Pi^P K^+)^{-1}, \tag{12}$$

where coupling constant K^+ and polarization function Π^P are 3×3 matrices

$$K^+ = \begin{pmatrix} K_0^+ & K_{03}^+ & K_{08}^+ \\ K_{30}^+ & K_3^+ & K_{38}^+ \\ K_{80}^+ & K_{83}^+ & K_8^+ \end{pmatrix}, \tag{13}$$

$$\Pi^P = \begin{pmatrix} \Pi_0^P & \Pi_{03}^P & \Pi_{08}^P \\ \Pi_{30}^P & \Pi_3^P & \Pi_{38}^P \\ \Pi_{80}^P & \Pi_{83}^P & \Pi_8^P \end{pmatrix}. \tag{14}$$

The matrix elements of coupling constant K^+ are written in Eq. (3), and the elements of polarization function Π^P are defined in Eq. (7) with index 3, 0, 8 denoting π_0, η_0, η_8, respectively. For convenience, we sometimes omit the argument $(k_0, \vec{k})$ in the polarization function and meson propagator.

We can obtain π_0, η, η' meson masses by solving the equation at $\vec{k} = \vec{0}$, where we neglect the width of mesons [35,41,42],

$$\det[\mathcal{M}^{-1}(k_0, \vec{0})] = 0. \tag{15}$$

The inverse of meson propagator matrix $\mathcal{M}$ can be simplified as

$$\mathcal{M}^{-1} = \frac{1}{2\det K^+}\begin{pmatrix} \mathcal{A} & \mathcal{B} & \mathcal{C} \\ \mathcal{B} & \mathcal{D} & \mathcal{E} \\ \mathcal{C} & \mathcal{E} & \mathcal{F} \end{pmatrix},$$
$$\begin{aligned}
\mathcal{A} &= (K_3^+ K_8^+ - K_{38}^{+2}) - 2\Pi_0^P \det K^+, \\
\mathcal{B} &= (K_{38}^+ K_{08}^+ - K_8^+ K_{03}^+) - 2\Pi_{03}^P \det K^+, \\
\mathcal{C} &= (K_{03}^+ K_{38}^+ - K_3^+ K_{08}^+) - 2\Pi_{08}^P \det K^+, \\
\mathcal{D} &= (K_0^+ K_8^+ - K_{08}^{+2}) - 2\Pi_3^P \det K^+, \\
\mathcal{E} &= (K_{03}^+ K_{08}^+ - K_0^+ K_{38}^+) - 2\Pi_{38}^P \det K^+, \\
\mathcal{F} &= (K_3^+ K_0^+ - K_{03}^{+2}) - 2\Pi_8^P \det K^+,
\end{aligned} \tag{16}$$

with

$$\begin{aligned}
\Pi_0^P &= \frac{2}{3}(\Pi_{uu}^P + \Pi_{dd}^P + \Pi_{ss}^P), \\
\Pi_3^P &= \Pi_{uu}^P + \Pi_{dd}^P, \\
\Pi_8^P &= \frac{1}{3}(\Pi_{uu}^P + \Pi_{dd}^P + 4\Pi_{ss}^P), \\
\Pi_{03}^P &= \Pi_{30}^P = \frac{\sqrt{6}}{3}(\Pi_{uu}^P - \Pi_{dd}^P), \\
\Pi_{08}^P &= \Pi_{80}^P = \frac{\sqrt{2}}{3}(\Pi_{uu}^P + \Pi_{dd}^P - 2\Pi_{ss}^P), \\
\Pi_{38}^P &= \Pi_{83}^P = \frac{\sqrt{3}}{3}(\Pi_{uu}^P - \Pi_{dd}^P),
\end{aligned} \tag{17}$$

and

$$\Pi_{ff}^P(k_0^2) = J_1^{(f)} - k_0^2 J_2^{(ff)}(k_0^2), \tag{18}$$

$$\begin{aligned}
J_2^{(ff)}(k_0^2) = -3\sum_l \alpha_l \frac{|Q_f B|}{2\pi}\int \frac{dp_z}{2\pi}\frac{1}{2E_f(4E_f^2 - k_0^2)} \\
\times\left(\tanh\frac{E_f + \mu}{2T} + \tanh\frac{E_f - \mu}{2T}\right).
\end{aligned} \tag{19}$$

Each matrix element in polarization function matrix Eq. (17) shows infrared divergence at $p_z = 0$ and $k_0 = 2\sqrt{m_f^2 + 2l|Q_f B|}$ with $f = u, d, s, l = 0, 1, 2, \ldots$, due to the integral term $\frac{1}{4E_f^2 - k_0^2}$. Because of the $\pi_0 - \eta - \eta'$ meson mixing, such infrared divergence will lead to several mass jumps for π_0, η, η' mesons, as shown in Figs. 3 and 4. Different from pion and kaon mesons, for η, η' mesons, we observe not only the mass jump at lowest Landau level $l = 0$ but also at a higher Landau level $l \neq 0$.

Because of the contact interaction in NJL model, the ultraviolet divergence cannot be eliminated through renormalization, and a proper regularization scheme is needed. In our work, we apply the Pauli-Villars regularization [33–35,42], which is gauge invariant and can guarantee the law of causality at finite magnetic field. By fitting the physical quantities, pion mass $m_\pi = 138$ MeV, pion decay constant $f_\pi = 93$ MeV, kaon mass $m_K = 495.7$ MeV, η'

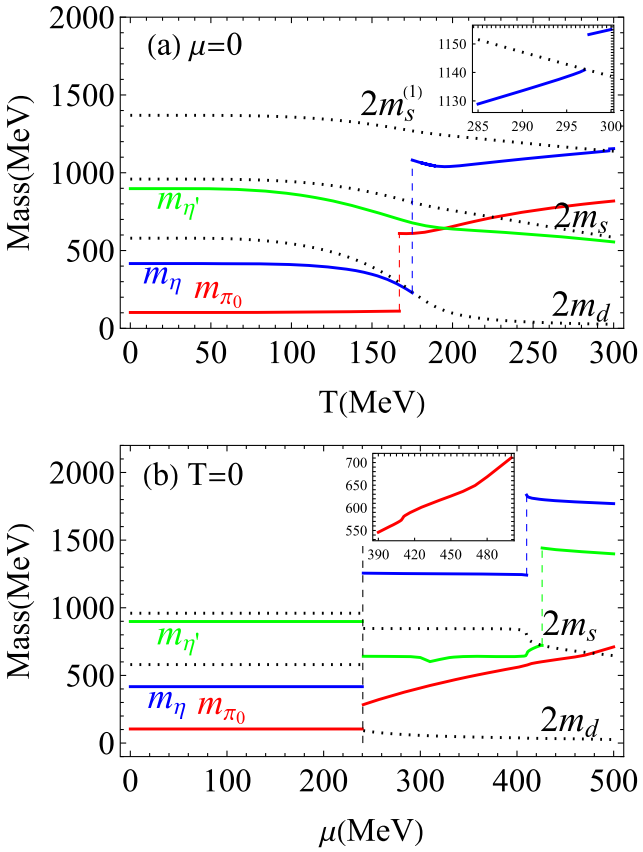

FIG. 3. Panel (a) shows the temperature dependence of π_0 (red solid lines), η (blue solid lines), η' (green solid lines) masses, and quark masses (black dotted lines) with $\mu = 0$ and $eB = 20m_\pi^2$. Panel (b) shows the quark chemical potential dependence of them at $T = 0$ and $eB = 20m_\pi^2$. The vertical dashed lines are used to denote the sudden mass jumps for quarks and mesons. The quark mass with a superscript "(l)" refers to the effective quark mass of the lth Landau level $m_f^{(l)} = \sqrt{m_f^2 + 2l|Q_f B|}$.

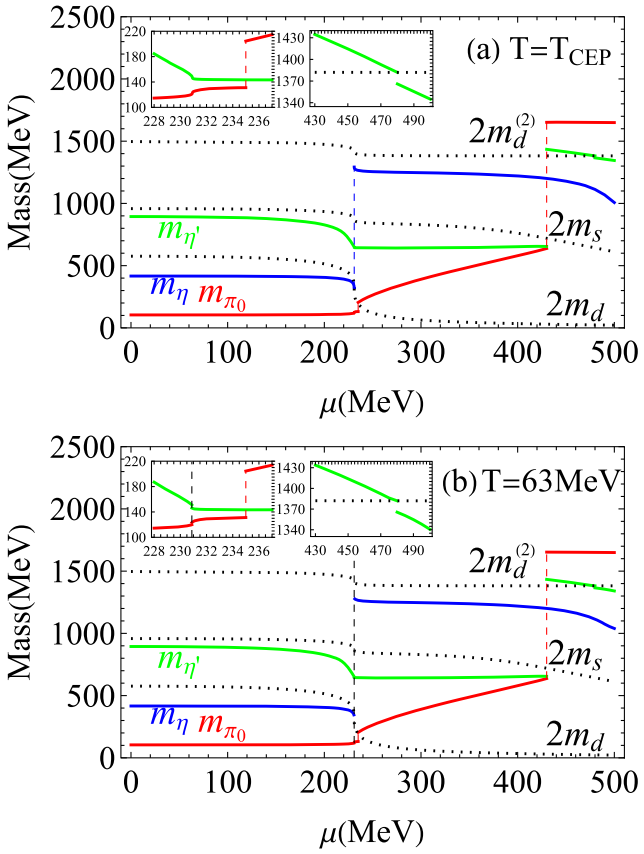

FIG. 4. Masses of π_0 (red solid lines), η (blue solid lines), η' (green solid lines), and quarks (black dotted lines) with $eB = 20m_\pi^2$ around the critical end point. In (a), we fixed the temperature at the CEP. Panel (b) is a case of the first order chiral phase transition near CEP. The vertical dashed lines are used to denote the sudden mass jumps for quarks and mesons. In the small figures at left side, we plot m_{π_0} in red and $m_{\eta'} - 500$ MeV in green. The quark mass with a superscript "(l)" refers to the effective quark mass of the lth Landau level $m_f^{(l)} = \sqrt{m_f^2 + 2l|Q_f B|}$.

meson mass $m_{\eta'} = 957.5$ MeV in vacuum, we fix the current masses of light quarks $m_0^u = m_0^d = 5.5$ MeV, and obtain the parameters $m_0^s = 154.7$ MeV, $G\Lambda^2 = 3.627$, $K\Lambda^5 = 92.835$, $\Lambda = 1101$ MeV. In the following numerical calculations, we fix magnetic field $eB = 20m_\pi^2$.

III. RESULTS AND ANALYSIS

Figure 1(a) plots the mass of K_0 meson m_{K_0} and the mass sum of the two constituent quarks $m_d + m_s$ as functions of temperature T at finite magnetic field $eB = 20m_\pi^2$ and vanishing quark chemical potential $\mu = 0$. To demonstrate the chiral symmetry restoration, we also plot light quark mass $2m_d$ and strange quark mass $2m_s$. The chiral symmetry restoration is a smooth crossover with $\mu = 0$, and the quark masses decrease continuously with the increase of temperature. As the Goldstone boson, the mass of K_0 meson monotonically increases with temperature before a sudden mass jump happens at the Mott transition temperature $T_{\rm Mott}^{K_0} = 140.0$ MeV, where the K_0 mass jumps from the bound state $m_{K_0} < m_d + m_s$ to the resonant state $m_{K_0} > m_d + m_s$. This mass jump is caused by the finite magnetic field, which leads to the dimension reduction of constituent quarks and the infrared divergence of the meson polarization function, as analyzed in Eq. (11). With $T > T_{\rm Mott}^{K_0}$, the mass of K_0 meson slightly decreases with temperature and then starts to rise at $T = 161.1$ MeV.

Figure 1(b) plots the mass of K_0 meson m_{K_0} and the mass sum of the two constituent quarks $m_d + m_s$ as functions of quark chemical potential μ at finite magnetic field $eB = 20m_\pi^2$ and vanishing temperature $T = 0$. To demonstrate the chiral symmetry restoration, we also plot light quark mass $2m_d$ and strange quark mass $2m_s$. The chiral symmetry restoration is a first order phase transition with increasing quark chemical potential and $T = 0$, and the quark masses show a jump at $\mu = 240.1$ MeV. This mass jump of constituent quarks also leads to the mass jump of K_0 meson. Since the K_0 mass jumps from $m_{K_0} < m_d + m_s$ to $m_{K_0} > m_d + m_s$, and satisfies the condition $m_{K_0} > 2\mu$, this is a Mott transition. In the chiral breaking phase with $\mu < 240.1$ MeV, the quark masses remain constant. After the chiral restoration phase transition, at $\mu = 410.2$ MeV, the strange quark mass decreases abruptly. For K_0 meson, the mass remains constant in the chiral breaking phase with $\mu < 240.1$ MeV, and increases in the chirally restored phase with $\mu > 240.1$ MeV. However, accompanied with the sudden change in the slope of the decreasing curve of strange quark mass, a fast decrease of K_0 mass happens around $\mu = 410.2$ MeV.

At finite temperature and quark chemical potential, there exists a critical end point of chiral symmetry restoration, which connects the crossover and the first order phase transition and is located at $(T_{\rm CEP}, \mu_{\rm CEP}) = (63.3, 230.9\ {\rm MeV})$ with $eB = 20m_\pi^2$. Figure 2 depicts the K_0 mass m_{K_0} and the mass sum of two constituent quarks $m_d + m_s$ around CEP. To demonstrate the chiral symmetry restoration, we also plot light quark mass $2m_d$ and strange quark mass $2m_s$. In Fig. 2(a), we fix temperature at CEP $T = T_{\rm CEP}$. The quark masses decrease with quark chemical potential, with the fastest change $\frac{dm_f}{d\mu} \to -\infty$ at $\mu = \mu_{\rm CEP}$. The K_0 mass increases with quark chemical potential, with the fastest change $\frac{dm_{K_0}}{d\mu} \to \infty$ at $\mu = \mu_{\rm CEP}$, too. At $\mu > \mu_{\rm CEP}$, the rate of increase in the K_0 mass becomes finite, and the Mott transition with K_0 mass jump happens at $\mu_{\rm Mott}^{K_0} = 231.5$ MeV $> \mu_{\rm CEP}$. At $\mu > \mu_{\rm Mott}^{K_0}$, K_0 mass continues to increase.

Around the CEP with $T > T_{\rm CEP}$, the chiral restoration is a smooth crossover, and the behavior of quark masses and K_0 mass is similar as in Fig. 2(a) but with finite slope of the mass curve. On the other side, as shown in Fig. 2(b) with

$T < T_{\mathrm{CEP}}$, the chiral restoration is a first order phase transition. The quark masses decrease with increasing quark chemical potential and jump in the quark mass (sum) occurs at $\mu = 230.96$ MeV. Accordingly, K_0 mass keeps increasing, and we observe two mass jumps, caused by the quark mass jump at $\mu = 230.96$ MeV and the magnetic field at $\mu = 231.5$ MeV, respectively. Comparing with Fig. 1, the nonmonotonical behavior of m_{K_0} disappears around CEP.

Figures 3 and 4 show the masses of π_0, η, η' mesons and the constituent quark masses at the lowest Landau level $2m_d, 2m_s$, and lth Landau level $2m_f^{(l)}$, at finite magnetic field, temperature and quark chemical potential. Since the u-quark mass is very close to (a little bit larger than) the d quark, to make the figure clear, we omit its lines. With finite magnetic field, the mixing of $\pi_0 - \eta - \eta'$ mesons leads to rich structures in their mass spectra.

In Fig. 3(a), with the continuous decreasing of the quark masses at finite temperature, π_0 mass increases slowly in the low temperature region $T < 167.0$ MeV and a mass jump from $m_{\pi_0} < 2m_d$ to $2m_d < m_{\pi_0} < 2m_s$ happens at $T = 167.0$ MeV. After that, π_0 mass slightly decreases and then starts to increase with temperature. When the π_0 mass crosses over the two times of the strange quark mass at high temperature, it increases smoothly, which indicates that the π_0 meson does not contain the strange quark, even with the $\pi_0 - \eta - \eta'$ mixing. For η meson, which contains the strange quark, its mass m_η decreases with temperature at $T < 175.0$ MeV. At $T = 175.0$ MeV, m_η jumps from $m_\eta < 2m_d$ to $m_\eta > 2m_s$. After that, m_η firstly decreases and later increases with temperature. At $T = 297.5$ MeV, another mass jump of η meson occurs, since m_η passes through the threshold of quark mass sum at a higher Landau level $2m_s^{(1)} = 2\sqrt{m_s^2 + 2|Q_s B|}$. η' meson is a resonant state in vacuum, which has the mass larger than two times of the d quark. With the increase of temperature, the mass of η' meson continuously decreases, and it becomes lower than π_0 mass at $T = 195.0$ MeV. In the whole temperature region, we observe $2m_d < m_{\eta'} < 2m_s$.

In Fig. 3(b), the first order chiral phase transition at $T = 0$ and $\mu = 240.1$ MeV leads to the mass jumps for quarks, and also causes the mass jumps of π_0, η, η' mesons. Before the mass jump, the mass of π_0, η, η' mesons remains their value in vacuum, respectively. At $\mu > 240.1$ MeV, π_0 mass increases with quark chemical potential. However, the increase slope changes abruptly at $\mu = 410.2$ MeV, where the strange quark mass abruptly decreases, and at $\mu = 478.2$ MeV, where the π_0 mass crosses over the two times of strange quark mass. This indicates that the π_0 meson is influenced by the strange quark, due to the mixing of $\pi_0 - \eta - \eta'$ mesons. For η meson, its mass jumps up from $m_\eta < 2m_d$ to $m_\eta > 2m_s$ at $\mu = 240.1$ MeV, and, after that, it decreases slightly. At $\mu = 410.2$ MeV, where the strange quark mass abruptly decreases, another mass jump of η meson happens, and then m_η goes down with quark chemical potential. η' meson is in a resonant state and its mass jumps down in association with the quark mass jump at $\mu = 240.1$ MeV. At $\mu = 426.0$ MeV, where the η' mass crosses over the strange quark mass two times, another mass jump from $m_{\eta'} < 2m_s$ to $m_{\eta'} > 2m_s$ happens. In the region 240.1 MeV $< \mu <$ 426.0 MeV, η' mass first decreases with quark chemical potential and then increases, with a local minimum at $\mu = 310.6$ MeV and the maximum increase slope at $\mu = 410.2$ MeV, where the strange quark mass decreases abruptly. At $\mu > 426.0$ MeV, the η' mass goes down with quark chemical potential.

Comparing Figs. 3(a) and 3(b), the structure of meson mass spectra behaves very differently, which demonstrates that the temperature and quark chemical potential have different effects on π_0, η, η' meson masses, respectively. Figure 4 depicts the situation near CEP, where panel (a) is at CEP and panel (b) represents an example of the first order chiral phase transition near CEP. To clearly show the near-CEP behavior of π_0 and η' at the same time, in the insets we plot m_{π_0} in red and $m_{\eta'} - 500$ MeV in green.

Figure 4(a) displays the masses of π_0, η, η' mesons and the quark masses at the lowest Landau level $2m_d, 2m_s$, and lth Landau level $2m_f^{(l)}$ at finite quark chemical potential with fixed magnetic field $eB = 20m_\pi^2$ and temperature $T = T_{\mathrm{CEP}}$. π_0 mass monotonically increases with quark chemical potential. The fastest change $\frac{dm_{\pi_0}}{d\mu} \to \infty$ is at $\mu = \mu_{\mathrm{CEP}}$, the first mass jump from $m_{\pi_0} < 2m_d$ to $2m_d < m_{\pi_0} < 2m_s$ happens at $\mu = 235.0$ MeV $> \mu_{\mathrm{CEP}}$, and another mass jump from $m_{\pi_0} < 2m_s$ to $m_{\pi_0} > 2m_s$ happens at $\mu = 430.0$ MeV. The mass of η meson decreases with the quark chemical potential, with the fastest change $\frac{dm_\eta}{d\mu} \to -\infty$ at $\mu = \mu_{\mathrm{CEP}}$ and a mass jump from $m_\eta < 2m_d$ to $m_\eta > 2m_s$ at $\mu = 230.96$ MeV $> \mu_{\mathrm{CEP}}$. The mass of η' meson also decreases with the quark chemical potential. Since it is in a resonant state, the mass decrease slope changes abruptly at $\mu = \mu_{\mathrm{CEP}}$. At $\mu = 430.0$ MeV, the mass of η' meson becomes degenerate with π_0 meson, and at the same time, the mass jump from $m_{\eta'} < 2m_s$ to $m_{\eta'} > 2m_s$ occurs. Another mass jump happens at $\mu = 480.1$ MeV, where the mass of η' meson passes through the threshold $2m_d^{(2)} = 2\sqrt{m_d^2 + 4|Q_d B|}$. Note that the mass ordering of π_0, η, η' meson varies, with $m_{\pi_0} < m_\eta < m_{\eta'}$ in the region $\mu < 230.96$ MeV, $m_{\pi_0} < m_{\eta'} < m_\eta$ in the region 230.96 MeV $< \mu <$ 430.0 MeV and $m_\eta < m_{\eta'} < m_{\pi_0}$ in the region $\mu > 430.0$ MeV, which are influenced by the meson mass jumps and the meson mixing under external magnetic field.

For the case of chiral crossover near CEP with $T > T_{\mathrm{CEP}}$, the behavior of π_0, η, η' meson mass is similar as in Fig. 4(a), but the infinite change slope of the mass of π_0, η meson is replaced by a finite value. For the case of first

order chiral phase transition near CEP with $T < T_{\mathrm{CEP}}$, as shown in Fig. 4(b), instead of the infinite change slope of π_0, η meson masses and the abrupt change of $m_{\eta'}$ decrease slope, we observe the mass jumps for the π_0, η, η' meson, caused by the mass jump of the constituent quarks at $\mu = 230.96$ MeV, and other behavior of π_0, η, η' meson masses looks similar as in Fig. 4(a).

IV. SUMMARY AND OUTLOOK

The mass spectra of neutral mesons K_0, π_0, η, η' on temperature-quark chemical potential (T-μ) plane in the presence of a constant magnetic field is studied in the $SU(3)$ NJL model.

As a Goldstone boson of chiral symmetry breaking, the mass of K_0 meson generally increases with temperature and/or quark chemical potential. At the Mott transition, an associated K_0 mass jump occurs. At vanishing T or μ, there exists nonmonotonical behavior of K_0 mass. Around the CEP, this behavior disappears, and we observe two K_0 meson mass jumps, one of which is induced by the mass jump of constituent quarks and occurs at a lower quark chemical potential and the other is induced by the magnetic field.

Due to the breaking of isospin symmetry between u and d quarks in magnetic fields, the mixing of $\pi_0 - \eta - \eta'$ mesons occurs and this leads to the rich structures of their mass spectra. The mass of π_0 meson increases with temperature and/or quark chemical potential, and, similarly to happens in the K_0 meson case, a mass jump occurs. In addition, π_0 mass is influenced by the strange quark because of the flavor mixing. This is demonstrated by the two changes in the slope of the quark chemical potential dependency of the π_0 mass at high μ and vanishing T (one motivated by the rapid change in m_s and the other by the crossing of the $2m_s$ threshold), as well as by the π_0 mass jump over the threshold $2m_s$ at finite T and μ. For the η meson, its mass mainly decreases with T and μ in the region without jumps. At vanishing μ, it shows two mass jumps caused by the magnetic field and nonmonotonical behavior appears after the first mass jump. At vanishing T, it shows two mass jumps that, in increasing order in quark chemical potential, are caused by the mass jump of constituent quarks and the magnetic field, respectively. Around the CEP, we observe one mass jump, and the nonmonotonical behavior disappears. For the η' meson, its mass continuously decreases at $\mu = 0$, but at $T = 0$, it displays two mass jumps and nonmonotonical behavior between them. Around the CEP, the η' meson mass jumps twice, induced by the constituent quark mass jump and by the magnetic field. The mass ordering of π_0, η, η' meson varies in medium.

As a consequence of such mass jumps, some interesting phenomena may result in relativistic heavy ion collisions where a strong magnetic field can be created. For instance, there might be a sudden enhancement or reduction of neutral meson production in medium, which will be studied in the future. It should be mentioned that we neglect the widths of mesons in our current calculations. At qualitative level, this approximation will not change the main structure of meson mass spectra. Its quantitative effect can be considered through the spectral function of mesons [110], which is under progress. The investigation of charged mesons, $K^{\pm}$ and $\pi^{\pm}$ mesons, and the consideration of inverse magnetic catalysis effect is also under progress and will be reported elsewhere.

ACKNOWLEDGMENTS

J. M. and S. M. are supported by the NSFC Grant No. 12275204 and Fundamental Research Funds for the Central Universities, and T. X. is supported by the NSFC Grant No. 61903371.

[1] C. Rosenzweig, J. Schechter, and C. G. Trahern, Phys. Rev. D **21**, 3388 (1980).
[2] C. M. Ko, Z. G. Wu, L. H. Xia, and G. E. Brown, Phys. Rev. Lett. **66**, 2577 (1991); **67**, 1811(E) (1991).
[3] G. Q. Li and G. E. Brown, Phys. Rev. C **58**, 1698 (1998).
[4] K. Paech, A. Dumitru, J. Schaffner-Bielich, H. Stoecker, G. Zeeb, D. Zschiesche, and S. Schramm, Acta Phys. Hung. A **21**, 151 (2004).
[5] H. T. Ding, S. T. Li, A. Tomiya, X. D. Wang, and Y. Zhang, Phys. Rev. D **104**, 014505 (2018).
[6] J. Rafelski and B. Muller, Phys. Rev. Lett. **36**, 517 (1976).
[7] D. E. Kharzeev, L. D. McLerran, and H. J. Warringa, Nucl. Phys. **A803**, 227 (2008).
[8] V. Skokov, A. Y. Illarionov, and T. Toneev, Int. J. Mod. Phys. A **24**, 5925 (2009).
[9] W. T. Deng and X. G. Huang, Phys. Rev. C **85**, 044907 (2012); Phys. Lett. B **742**, 296 (2015).
[10] K. Tuchin, Adv. High Energy Phys. **2013**, 490495 (2013).
[11] N. Agasian and I. Shushpanov, J. High Energy Phys. 10 (2001) 006.
[12] G. Colucci, E. Fraga, and A. Sedrakian, Phys. Lett. B **728**, 19 (2014).
[13] J. Anderson, J. High Energy Phys. 10 (2012) 005; Phys. Rev. D **86**, 025020 (2012).
[14] K. Kamikado and T. Kanazawa, J. High Energy Phys. 03 (2014) 009.
[15] G. Krein and C. Miller, Symmetry **13**, 551 (2021).

[16] A. Ayala, J. L. Hernández, L. A. Hernández, R. L. S. Farias, and R. Zamora, Phys. Rev. D **103**, 054038 (2021).
[17] R. M. Aguirre, Phys. Rev. D **96**, 096013 (2017).
[18] A. Ayala, R. L. S. Farias, S. Hernández-Ortiz, L. A. Hernández, D. M. Paret, and R. Zamora, Phys. Rev. D **98**, 114008 (2018).
[19] A. Das and N. Haque, Phys. Rev. D **101**, 074033 (2020).
[20] A. N. Tawfik, A. M. Diab, and T. M. Hussein, Chin. Phys. C **43**, 034103 (2019).
[21] Y. Hidaka and A. Yamatomo, Phys. Rev. D **87**, 094502 (2013).
[22] E. Luschevskaya, O. Solovjeva, O. Kochetkov, and O. Teryaev, Nucl. Phys. **B898**, 627 (2015).
[23] E. Luschevskaya, O. Solovjeva, and O. Teryaev, Phys. Lett. B **761**, 393 (2016).
[24] G. S. Bali, B. Brandt, G. Endrődi, and B. Gläßle, Phys. Rev. D **97**, 034505 (2018).
[25] G. S. Bali, B. Brandt, G. Endrődi, and B. Gläßle, Proc. Sci. LATTICE2015 (**2016**) 265.
[26] G. S. Bali, F. Bruckmann, G. Endrődi, Z. Fodor, S. D. Katz, S. Krieg, A. Schäfer, and K. K. Szabó, J. High Energy Phys. 02 (2012) 044.
[27] H. T. Ding, S. T. Li, A. Tomiya, X. D. Wang, and Y. Zhang, Phys. Rev. D **104**, 014505 (2021).
[28] S. Klevansky, Rev. Mod. Phys. **64**, 649 (1992).
[29] S. Avancini, R. Farias, M. Pinto, W. Travres, and V. Timóteo, Phys. Lett. B **767**, 247 (2017).
[30] S. Avancini, W. Travres, and M. Pinto, Phys. Rev. D **93**, 014010 (2016).
[31] S. Fayazbakhsh, S. Sadeghian, and N. Sadooghi, Phys. Rev. D **86**, 085042 (2012).
[32] S. Fayazbakhsh and N. Sadooghi, Phys. Rev. D **88**, 065030 (2013).
[33] S. J. Mao, Phys. Lett. B **758**, 195 (2016).
[34] S. J. Mao, Phys. Rev. D **94**, 036007 (2016).
[35] S. J. Mao and Y. X. Wang, Phys. Rev. D **96**, 034004 (2017).
[36] Z. Y. Wang and P. F. Zhuang, Phys. Rev. D **97**, 034026 (2018).
[37] M. Coppola, D. Dumm, and N. Scoccola, Phys. Lett. B **782**, 155 (2018).
[38] R. Zhang, W. J. Fu, and Y. X. Liu, J. Eur. Phys. C **76**, 307 (2016).
[39] H. Liu, X. Wang, L. Yu, and M. Huang, Phys. Rev. D **97**, 076008 (2018).
[40] D. N. Li, G. Q. Cao, and L. Y. He, Phys. Rev. D **104**, 074026 (2021).
[41] S. J. Mao, Phys. Rev. D **99**, 056005 (2019).
[42] L. Y. Li and S. J. Mao, Chin. Phys. C **46**, 094105 (2022).
[43] B. K. Sheng, Y. Y. Wang, X. Y. Wang, and L. Yu, Phys. Rev. D **103**, 094001 (2021).
[44] D. G. Dumm, M. I. Villafañe, and N. N. Scoccola, Phys. Rev. D **97**, 034025 (2018).
[45] S. S. Avancini, R. L. S. Farias, and W. R. Tavares, Phys. Rev. D **99**, 056009 (2019).
[46] N. Chaudhuri, S. Ghosh, S. Sarkar, and P. Roy, Phys. Rev. D **99**, 116025 (2019).
[47] M. Coppola, D. G. Dumm, S. Noguera, and N. N. Scoccola, Phys. Rev. D **100**, 054014 (2019).
[48] J. Y. Chao, Y. X. Liu, and L. Chang, arXiv:2007.14258.
[49] K. Xu, J. Y. Chao, and M. Huang, Phys. Rev. D **103**, 076015 (2021).
[50] V. D. Orlovsky and Y. A. Simonov, J. High Energy Phys. 09 (2013) 136.
[51] K. Hattori, T. Kojo, and N. Su, Nucl. Phys. **A951**, 1 (2016).
[52] M. A. Andreichikov, B. O. Kerbikov, E. V. Luschevskaya, Y. A. Simonov, and O. E. Solovjeva, J. High Energy Phys. 05 (2017) 007.
[53] Y. A. Simonov, Yad. Fiz. **79**, 277 (2016) [Phys. At. Nucl. **79**, 455 (2016)].
[54] M. A. Andreichikov and Y. A. Simonov, Eur. Phys. J. C **78**, 902 (2018).
[55] C. A. Dominguez, M. Loewe, and C. Villavicencio, Phys. Rev. D **98**, 034015 (2018).
[56] M. N. Chernodub, Phys. Rev. D **82**, 085011 (2010).
[57] M. N. Chernodub, Phys. Rev. Lett. **106**, 142003 (2011).
[58] N. Callebaut, D. Dudal, and H. Verschelde, Proc. Sci. FACESQCD2010 (**2010**) 046 [arXiv:1102.3103].
[59] M. Ammon, J. Erdmenger, P. Kerner, and M. Strydom, Phys. Lett. B **706**, 94 (2011).
[60] R. G. Cai, S. He, L. Li, and L. F. Li, J. High Energy Phys. 12 (2013) 036.
[61] M. Frasca, J. High Energy Phys. 11 (2013) 099.
[62] M. A. Andreichikov, B. O. Kerbikov, V. D. Orlovsky, and Y. A. Simonov, Phys. Rev. D **87**, 094029 (2013).
[63] H. Liu, L. Yu, and M. Huang, Phys. Rev. D **91**, 014017 (2015).
[64] H. Liu, L. Yu, and M. Huang, Chin. Phys. C **40**, 023102 (2016).
[65] H. Liu, L. Yu, M. Chernodub, and M. Huang, Phys. Rev. D **94**, 113006 (2016).
[66] M. Kawaguchi and S. Matsuzaki, Phys. Rev. D **93**, 125027 (2016).
[67] S. Ghosh, A. Mukherjee, M. Mandal, S. Sarkar, and P. Roy, Phys. Rev. D **94**, 094043 (2016).
[68] S. Ghosh, A. Mukherjee, M. Mandal, S. Sarkar, and P. Roy, Phys. Rev. D **96**, 116020 (2017).
[69] O. Larina, E. Luschevskaya, O. Kochetkov, and O. V. Teryaev, Proc. Sci. LATTICE2014 (**2014**) 120.
[70] E. V. Luschevskaya, O. A. Kochetkov, O. V. Teryaev, and O. E. Solovjeva, JETP Lett. **101**, 674 (2015).
[71] H. T. Ding, S. T. Li, S. Mukherjee, A. Tomiya, and X. D. Wang, Proc. Sci. LATTICE2019 (**2020**) 250.
[72] S. Ghosh, A. Mukherjee, N. Chaudhuri, P. Roy, and S. Sarkar, Phys. Rev. D **101**, 056023 (2020).
[73] T. Kojo, Eur. Phys. J. A **57**, 317 (2021).
[74] A. Mishra and S. Misra, Int. J. Mod. Phys. E **30**, 2150014 (2021).
[75] S. S. Avancini, M. Coppola, N. N. Scoccola, and J. C. Sodré, Phys. Rev. D **104**, 094040 (2021).
[76] X. L. Sheng, S. Y. Yang, Y. L. Zou, and D. F. Hou, arXiv:2209.01872.
[77] K. Marasinghe and K. Tuchin, Phys. Rev. C **84**, 044908 (2011).
[78] C. S. Machado, F. S. Navarra, E. G. de Oliveira, J. Noronha, and M. Strickland, Phys. Rev. D **88**, 034009 (2013).
[79] J. Alford and M. Strickland, Phys. Rev. D **88**, 105017 (2013).
[80] C. S. Machado, S. I. Finazzo, R. D. Matheus, and J. Noronha, Phys. Rev. D **89**, 074027 (2014).

[81] S. Cho, K. Hattori, S. H. Lee, K. Morita, and S. Ozaki, Phys. Rev. Lett. **113**, 172301 (2014).
[82] S. Cho, K. Hattori, S. H. Lee, K. Morita, and S. Ozaki, Phys. Rev. D **91**, 045025 (2015).
[83] D. Dudal and T. G. Mertens, Phys. Rev. D **91**, 086002 (2015).
[84] C. Bonati, M. D'Elia, and A. Rucci, Phys. Rev. D **92**, 054014 (2015).
[85] P. Gubler, K. Hattori, S. H. Lee, M. Oka, S. Ozaki, and K. Suzuki, Phys. Rev. D **93**, 054026 (2016).
[86] T. Yoshida and K. Suzuki, Phys. Rev. D **94**, 074043 (2016).
[87] P. Sushruth Reddy, C. S. Amal Jahan, Nikhil Dhale, Amruta Mishra, and J. Schaffner-Bielich, Phys. Rev. C **97**, 065208 (2018).
[88] A. Mishra, A. Jahan CS, S. Kesarwani, H. Raval, S. Kumar, and J. Meena, Eur. Phys. J. A **55**, 99 (2019).
[89] B. C. Tiburzi, Nucl. Phys. **A814**, 74 (2008).
[90] M. A. Andreichikov, B. O. Kerbikov, V. D. Orlovsky, and Y. A. Simonov, Phys. Rev. D **89**, 074033 (2014).
[91] B. C. Tiburzi, Phys. Rev. D **89**, 074019 (2014).
[92] A. Haber, F. Preis, and A. Schmitt, AIP Conf. Proc. **1701**, 080010 (2016).
[93] B. R. He, Phys. Lett. B **765**, 109 (2017).
[94] A. Deshmukh and B. C. Tiburzi, Phys. Rev. D **97**, 014006 (2018).
[95] U. Yakhshiev, H. C. Kim, and M. Oka, Phys. Rev. D **99**, 054027 (2019).
[96] Y. Nambu and G. Jona-Lasinio, Phys. Rev. **122**, 345 (1961); **124**, 246 (1961).
[97] M. Volkov, Phys. Part. Nucl. **24**, 35 (1993).
[98] T. Hatsuda and T. Kunihiro, Phys. Rep. **247**, 221 (1994).
[99] M. Buballa, Phys. Rep. **407**, 205 (2005).
[100] P. Rehberg, S. P. Klevansky, and J. Hüfner, Phys. Rev. C **53**, 410 (1996).
[101] T. Kunihiro and T. Hatsuda, Phys. Lett. B **206**, 385 (1988).
[102] V. Bernard, R. L. Jaffe, and U. G. Meissner, Nucl. Phys. **B308**, 753 (1988).
[103] H. Reinhardt and R. Alkofer, Phys. Lett. B **207**, 482 (1988).
[104] G. 't Hooft, Phys. Rev. D **14**, 3432 (1976).
[105] G. 't Hooft, Phys. Rep. **142**, 357 (1986).
[106] N. F. Mott, Rev. Mod. Phys. **40**, 677 (1968).
[107] P. Zhuang, J. Hüfner, and S. P. Klevansky, Nucl. Phys. **A576**, 525 (1994).
[108] J. Huefner, S. Klevansky, and P. Rehberg, Nucl. Phys. **A606**, 260 (1996).
[109] P. Costa, M. Ruivo, and Y. Kalinovsky, Phys. Lett. B **560**, 171 (2003).
[110] T. Xia, J. Hu, and S. J. Mao, Chin. Phys. C **43**, 054103 (2019).